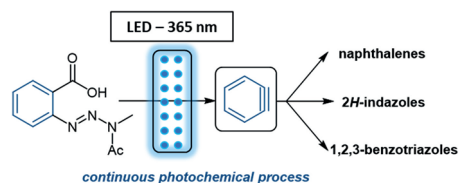


# Development of a Continuous Photochemical Benzyne-Forming Process

Cormac Bracken<sup>a</sup>   
 Andrei S. Batsanov<sup>b</sup>   
 Marcus Baumann<sup>\*a</sup>

<sup>a</sup> School of Chemistry, University College Dublin, Science Centre South, D04 N2E2, Dublin, Ireland  
 marcus.baumann@ucd.ie

<sup>b</sup> Department of Chemistry, University of Durham, South Road, DH1 3LE, Durham, UK



Received: 23.12.2020

Accepted after revision: 07.01.2021

Published online: 01.02.2021

DOI: 10.1055/s-0040-1706016; Art ID: so-2020-d0048-op



License terms:

© 2021. The Author(s). This is an open access article published by Thieme under the terms of the Creative Commons Attribution-NonDerivative-NonCommercial-License, permitting copying and reproduction so long as the original work is given appropriate credit. Contents may not be used for commercial purposes or adapted, remixed, transformed or built upon. (<https://creativecommons.org/licenses/by-nc-nd/4.0/>)

**Abstract** A continuous-flow process is presented that enables the safe generation and derivatization of benzyne under photochemical conditions. This is facilitated by a new high-power LED lamp emitting light at 365 nm. The resulting flow process effectively controls the release of gaseous by-products based on an adjustable backpressure regulator and delivers a series of heterocyclic products in a short residence time of 3 minutes. The robustness of this methodology is demonstrated for the rapid generation of benzotriazoles, 2H-indazoles and various furan-derived adducts, facilitating the preparation of these important heterocyclic scaffolds via a simple and readily scalable flow protocol.

**Key words** flow chemistry, photochemistry, benzyne, cycloadditions, high-energy intermediates, reaction development, heterocycles

Continuous-flow chemistry is now a well-established enabling technology that provides multiple benefits arising from reactor miniaturization, such as improved heat and mass transfer. This allows chemists to exploit a vast variety of transformations that are difficult to control in batch mode.<sup>1</sup> The creation of fleeting high-energy intermediates and their effective trapping is thereby a prime example that is exploited in many organometallic transformations such as lithiation processes.<sup>2</sup>

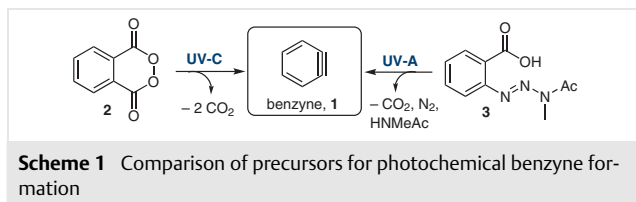
More recently, the development of continuous light-driven reactions has showcased the effective implementation of flow chemistry for a variety of important photochemical transformations.<sup>3</sup> The design of different flow reactors thereby enables applications based on both visible

light LEDs as well as traditional UV lamps to create a multitude of important chemical entities.<sup>4</sup> In view of the industrial applications, photochemical transformations are gaining momentum as photons are seen as traceless and tunable reagents, and recent reports on the scalability of continuous photochemical processes<sup>3c,5</sup> including those towards drugs like artemisinin<sup>6</sup> have highlighted the potential for their exploitation.

Given the salient features of flow chemistry, a class of important transformations that is noticeably underutilized, concerns the generation and use of benzyne.<sup>7</sup> While Kobayashi's mild method starting from *ortho*-TMS aryl triflates<sup>8</sup> is one of the most exploited strategies for accessing benzyne, alternatives based on diazotization and subsequent fragmentation of anthranilic acid derivatives or by *ortho*-lithiation of halobenzenes, have been used.<sup>9</sup> Although the last decades have witnessed impressive applications of especially Kobayashi's method, which include various studies towards heteroarynes,<sup>10</sup> the generation and use of benzyne is not a commonly exploited strategy. This may point to the necessity for generating bespoke substrates (e.g., TMS-aryl triflates) that require fluoride as an activation reagent to trigger benzyne formation, as well as concerns regarding scale-up of the exothermic benzyne forming process.

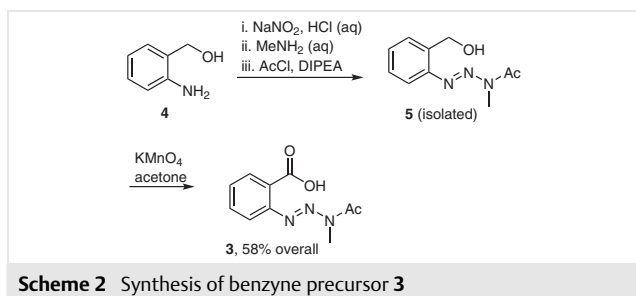
We were thus intrigued by the opportunity to develop a continuous light-driven benzyne forming reaction that would overcome some of these limitations. Crucially, such a continuous approach would effectively exploit the benefits of flow chemistry, thereby rendering a robust method to enable and stimulate further developments in this important area of research.

Upon surveying the literature, we identified two suitable precursors that would render the desired benzyne species **1** upon irradiation with UV light (Scheme 1).



Phthaloyl peroxide **2** is known to be a suitable benzyne precursor with recent exploitations demonstrating its use towards the creation of benzotriazoles.<sup>11</sup> Benzoic acid derived triazine **3** was initially reported as a photolysis product from nitro benzaldehyde *N*-acylhydrazones that would subsequently generate benzyne.<sup>12</sup> Whilst both species would generate benzyne accompanied by liberation of gaseous by-products (CO<sub>2</sub> and N<sub>2</sub>), we decided to exploit the latter option as a recent report by Schnarr<sup>13</sup> outlines the use of milder UV-A light in combination with short reaction times, which appeared preferable in view of broader substrate scope and fast reactions.

Following the reported synthesis<sup>13</sup> of triazine species **3** that exploits diazotization of 2-aminobenzylalcohol (**4**), sequential trapping of the diazonium intermediate with methyl amine and acetyl chloride and final oxidation to render the carboxylic acid, we were able to access gram quantities of this building block (Scheme 2). Pleasingly, we were able to increase the overall yield of **3** by ca. 20% by modifying the isolation and purification process slightly (see below).



Despite prior studies on this structure towards formation of benzyne, we were surprised by the lack of detailed characterization that would determine its suitability towards photochemical benzyne formation. To this end, we first recorded the UV/Vis spectrum of **3**, which showed a maximum absorbance at 288 nm extending as anticipated as far as 370 nm (UV-A; Figure 1). This provided valuable information regarding the choice of light source in subsequent studies.

In addition, single crystals of **3** were obtained by slow evaporation of a sample solution (in DCM) allowing us to analyze its molecular structure by X-ray diffraction (Figure 2). This structure<sup>14</sup> reveals a hydrogen bond in the solid state between the carboxyl group and the triazene moiety,

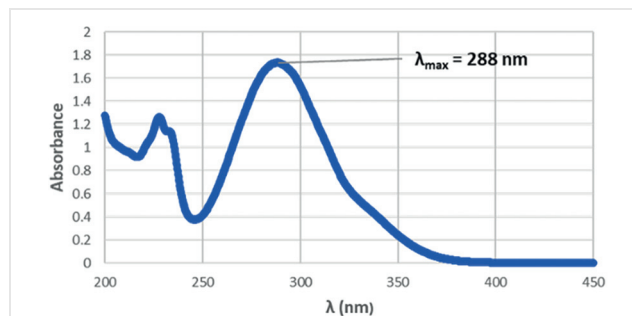


**Figure 1** UV/Vis spectrum of benzyne precursor **3** (MeCN)

locking the conformation of this entity. Furthermore, this results in planarity for the entire scaffold, enabling efficient light absorption due to extended  $\pi$ -conjugation, which mirrors the information observed in the UV/Vis spectrum of **3**.

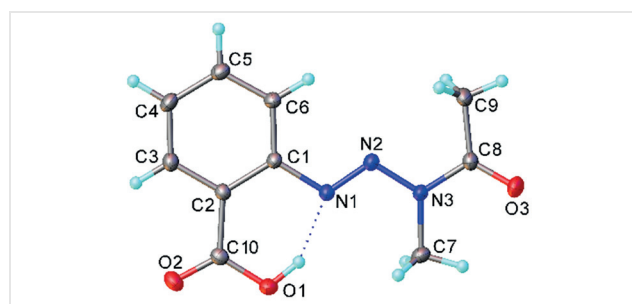
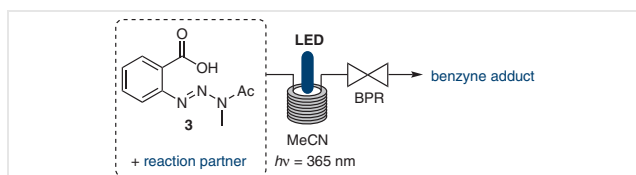


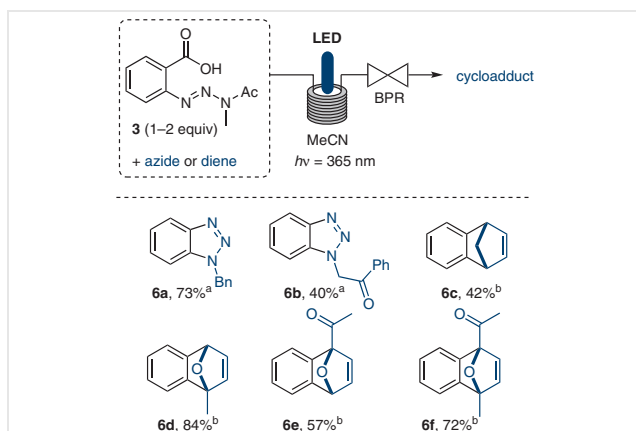
**Figure 2** Molecular structure of **3**

We next turned our attention to the development of a continuous-flow process that would exploit a photochemical reactor to generate the benzyne intermediate in the presence of various trapping agents. Specifically, we felt that flow processing would provide a superior approach, as the gaseous by-products are released safely and steadily (facilitated by using a backpressure regulator, BPR), whilst the uniform irradiation in combination with excellent temperature control and reaction automation are key features for future scale-up to create gram quantities of products. Based on our group's prior studies exploiting continuous photochemical approaches, we opted to utilize a Vapourtec E-series flow platform in combination with a tunable high-power LED (2 panels, 25–50 W each) emitting light at 365 nm.<sup>15</sup> The LED is thereby placed at the center of a flow coil reactor (10 mL, FEP) and the two LED panels can be operated either separately or in combination, depending on the specific application (see the Supporting Information for photographic details). Temperature control is achieved by directing a stream of chilled gas (N<sub>2</sub> or compressed air) into the encased reactor system. Upon exiting this setup, the reaction mixture passes an adjustable BPR (0–10 bar) prior to collection (Scheme 3).



**Scheme 3** Flow reactor setup for continuous benzyne formation

As depicted in Scheme 3, the benzyne precursor **3** and the desired reaction partner would be premixed as no reaction takes place in the absence of UV-light. To replicate the synthesis of previously reported benzotriazoles,<sup>13</sup> which are versatile scaffolds of biological relevance,<sup>16</sup> we prepared a solution of azide substrate (2 equiv) and benzyne precursor **3** (1 equiv, MeCN, 0.05 M) and pumped this into the high-power LED reactor to optimize power setting, temperature, and residence time. Pleasingly, it was quickly found that both benzyl azide and phenacetyl azide were competent reaction partners that generated the desired benzotriazole targets **6a** and **6b** within a short residence times of 3 minutes (Scheme 4). To minimize thermal degradation and potential over-irradiation, the reactor temperature was maintained at ca. 28 °C whilst limiting the LED power to 37.5 W using only one panel of LEDs. Due to the formation of gaseous by-products (CO<sub>2</sub> and N<sub>2</sub>) during the benzyne forming step, a slug-flow pattern was observed in the tubing. Separation of these gases was achieved upon collection of the crude product after passing a BPR (ca. 2 bar).



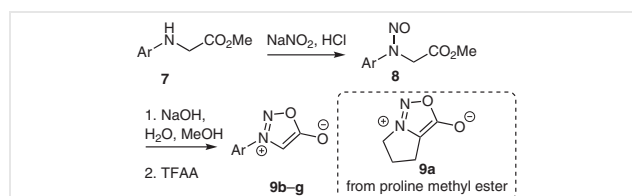
**Scheme 4** Flow synthesis of benzotriazoles and other cycloadducts; <sup>a</sup> 1.0 equiv of **3**; <sup>b</sup> 2.0 equiv of **3**.

To further exploit this continuous photochemical benzyne forming process, we wished to also study a set of cyclic dienes as reaction partners. We thus selected cyclopentadiene and various furans and subjected their solutions with **3** (MeCN, 50 mM) to our flow process. As indicated through initial test reactions, higher yields of the corresponding cycloadducts **6c–f** were achieved when using an

excess of **3** (2 equiv). As before, the use of the LED emitting at 365 nm was key to the successful synthesis of the desired cycloadducts and enabled fast reactions through a short residence time of 3 minutes.

Having demonstrated proof of concept, we next wished to evaluate our method for the synthesis of 2*H*-indazoles that are frequently exploited heterocycles in medicinal chemistry programs.<sup>17</sup> As their conventional synthesis relies on multistep routes, we felt that a flow process could streamline this effort. Specifically, we wished to utilize sydnone<sup>18</sup> as readily accessible mesoionic reaction partners that would initially undergo a formal [3+2]-cycloaddition with benzyne, followed by [4+2]-cycloreversion. The release of gaseous CO<sub>2</sub> would thereby be easily accommodated within our flow process.

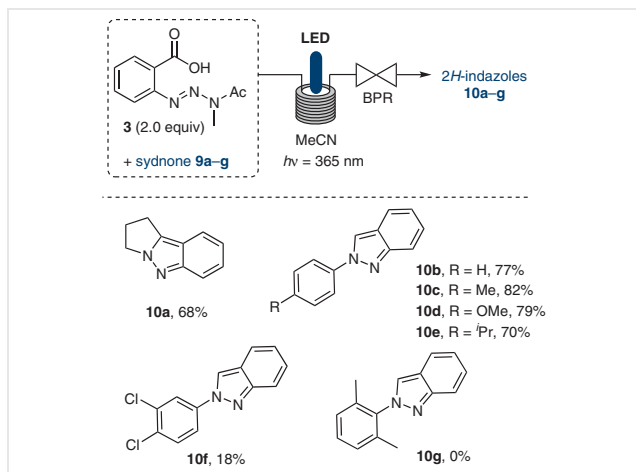
The synthesis of the sydnone was accomplished by following literature precedent,<sup>18</sup> converting *N*-phenyl glycine derivatives and proline methyl ester via *N*-nitrosated intermediates (**8**) into the corresponding building blocks (Scheme 5, see the Supporting Information for details).



**Scheme 5** Synthesis of sydnone **9a–g**

With a small selection of sydnone on hand, we next embarked on their transformation into 2*H*-indazoles. As before, a stock solution of benzyne precursor (**3**, 2 equiv, 0.1 M MeCN) and sydnone (1 equiv) was prepared and pumped through the photoreactor (365 nm, 37.5 W) with a residence time of 3 minutes. Pleasingly, the formation of several 2*H*-indazoles was achieved in isolated yields up to 82% (Scheme 6). Whilst the proline derived sydnone (**9a**) and various electron-rich aryl appendages on the sydnone precursor enabled high yields (68–82%), we noticed that electron-withdrawing substituents (e.g., 3,4-dichlorophenyl) reduced the yield significantly.<sup>19</sup> Furthermore, using 2,6-dimethylphenyl-substituted sydnone, no 2*H*-indazole product (**10g**) was observed. Whilst unexpected at first, we surmise that this substitution pattern leads to twisting of both rings, as indicated by a significant drop in the UV-absorbance (see the Supporting Information for details). The loss of conjugation arising from this conformational change thus appears to cause the observed reaction outcome.

To test the robustness and scalability of this flow process towards the creation of 2*H*-indazole species, we selected proline derived sydnone **9a** as the substrate and processed 760 mg through our LED flow reactor. Pleasingly, this resulted in the generation of 648 mg of the desired target



**Scheme 6** Flow synthesis of 2*H*-indazoles **10a–g** via benzyne cyclo-addition cascade

(68% yield) with a throughput of 4.4 mmol/h. Furthermore, we secured single crystals of product **10a** allowing us to verify its anticipated molecular structure by means of X-ray diffraction (Figure 3).<sup>20</sup>

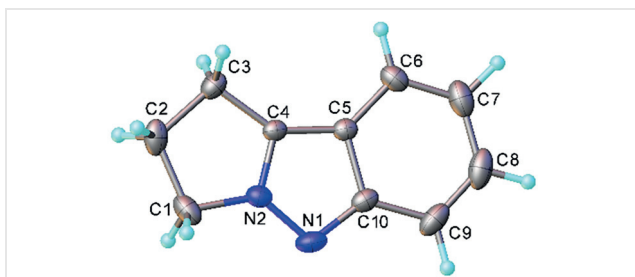


**Figure 3** Molecular structure of **10a**

In conclusion, we have developed a versatile flow protocol for the photochemical generation and concurrent trapping of benzyne from a stable and readily accessible triazine precursor. Crucially, the tunable high-power LED light source<sup>21</sup> provided for uniform irradiation at 365 nm and rendered a variety of important drug-like heterocycles in short residence times and in high yields. Lastly, the scalability of this flow process has been demonstrated, enabling and facilitating future exploitations of continuous benzyne-based transformations.

Solvents were purchased from Sigma–Aldrich and used without further purification. Substrates and reagents were purchased from Alfa Aesar, Fischer, Fluorochem or Sigma–Aldrich and used as received. <sup>1</sup>H NMR spectra were recorded with 400 and 600 MHz instruments and are reported relative to residual solvent: CHCl<sub>3</sub> (δ = 7.26 ppm). <sup>13</sup>C NMR spectra were recorded with the same instruments (100 and 151 MHz) and again are reported relative to CHCl<sub>3</sub> (δ = 77.16 ppm). Data reported for <sup>1</sup>H NMR are as follows: chemical shift (δ/ppm) (multi-

plicity, coupling constant (Hz), integration). Multiplicities are reported as follows: s = singlet, d = doublet, t = triplet, q = quartet, p = pentet, h = heptet, m = multiplet. Data for <sup>13</sup>C{<sup>1</sup>H} NMR are reported in terms of chemical shift (δ/ppm) and multiplicity (C, CH, CH<sub>2</sub>, or CH<sub>3</sub>). COSY, HSQC and HMBC, experiments were used in the structural assignment. IR spectra were recorded with a Bruker Platinum spectrophotometer (neat, ATR sampling) with the intensities of the characteristic signals being reported as weak (w, <20% of the tallest signal), medium (m, 21–70% of the tallest signal), or strong (s, >71% of the tallest signal). High-resolution mass spectrometry (HRMS) was performed using the indicated techniques with a micromass LCT orthogonal time-of-flight mass spectrometer with leucine-enkephalin (Tyr-Gly-Phe-Leu) as an internal lock mass. For UV/Vis measurements, a Shimadzu UV-1800 UV spectrophotometer was used. Melting points were recorded with a Stuart SMP10 melting point apparatus and are uncorrected. Continuous-flow experiments were performed with a Vapourtec E-Series system equipped with a UV150 photoreactor in combination with a high-power LED emitting light at 365 nm wavelength.

#### Synthesis of (*E*)-2-(3-Acetyl-3-methyltriaz-1-en-1-yl)benzoic Acid (**3**)<sup>13</sup>

A suspension of 2-aminobenzyl alcohol (600 mg, 4.8 mmol, 1.00 equiv) in H<sub>2</sub>O (4 mL) was stirred at 0 °C. Concd HCl (2.4 mL, 29 mmol, 6.00 equiv) was added slowly, resulting in an orange solution. NaNO<sub>2</sub> (342 mg, 4.9 mmol, 1.03 equiv) in H<sub>2</sub>O (1 mL) was subsequently added dropwise and the orange solution was stirred for a further 20 minutes before being added dropwise to a stirred solution of MeNH<sub>2</sub> (40% in H<sub>2</sub>O, 7.2 mL, 92.2 mmol, 19.2 equiv) at –25 °C. The reaction mixture was extracted immediately upon complete addition of the diazonium solution with EtOAc (2 × 40 mL). The organic phases were then washed with sodium bicarbonate (40 mL), brine (40 mL) and dried over Na<sub>2</sub>SO<sub>4</sub>. The solution was then concentrated in vacuo, providing a red/orange oil, which was used in the next step without further purification.

CH<sub>2</sub>Cl<sub>2</sub> (50 mL) was added to the red/orange oil and the solution stirred at 0 °C before Huenig's base was added (3.3 mL, 19.2 mmol, 4.0 equiv). AcCl (0.34 mL, 4.8 mmol, 1.0 equiv) was then added slowly and the solution was stirred for 2.5 h. The reaction mixture was then diluted with CH<sub>2</sub>Cl<sub>2</sub> and acidified to pH 4–5 with 1 M HCl. The organic phase was separated, washed with brine (40 mL), dried over Na<sub>2</sub>SO<sub>4</sub>, and then concentrated to provide an orange oil that solidified to give an orange solid that was used without further purification. The orange solid was dissolved in acetone (50 mL) and stirred at room temperature. KMnO<sub>4</sub> (1.07 g, 6.78 mmol, 1.4 equiv) was added in portions and the reaction was stirred for a further 3.5 h. Na<sub>2</sub>SO<sub>3</sub> (sat. aq.) was added in 2–3 mL portions until the purple color disappeared. The reaction solution was diluted with CH<sub>2</sub>Cl<sub>2</sub> (50 mL), and the solution was acidified to pH 4–5 with 1 M HCl. The organic phase was then separated before being washed with brine (40 mL) and dried over Na<sub>2</sub>SO<sub>4</sub>. The reaction mixture was then concentrated in vacuo to provide **3** as a light-brown solid. The solid was cooled before being triturated from Et<sub>2</sub>O and filtered under suction to yield (*E*)-2-(3-acetyl-3-methyltriaz-1-en-1-yl)benzoic acid (616 mg, 2.8 mmol, 58 %) (**3**) as a dark-yellow solid (mp 160–162 °C).

IR (neat): 2917 (w), 2734 (w), 1715 (s), 1594 (m), 1484 (m), 1464 (m), 1420 (m) cm<sup>-1</sup>.

<sup>1</sup>H NMR (CDCl<sub>3</sub>, 400 MHz): δ = 8.34 (d, *J* = 8.0 Hz, 1 H), 7.76 (d, *J* = 8.0 Hz, 1 H), 7.66–7.62 (m, *J* = 8.0 Hz, 1 H), 7.55–7.51 (m, *J* = 8.0 Hz, 1 H), 3.51 (s, 3 H), 2.64 (s, 3 H).

$^{13}\text{C}$  NMR ( $\text{CDCl}_3$ , 101 MHz):  $\delta = 172.4$  (C), 165.9 (C), 146.3 (C), 133.9 (C), 133.1 (CH), 130.0 (CH), 125.1 (CH), 116.6 (CH), 28.5 ( $\text{CH}_3$ ), 22.0 ( $\text{CH}_3$ ).

HRMS (TOF-ESI+):  $m/z$  [ $\text{M} + \text{H}$ ] $^+$  calcd for  $\text{C}_{10}\text{H}_{12}\text{N}_3\text{O}_3$ : 222.0873; found: 222.0869.

UV/Vis ( $\lambda_{\text{max}}$ , MeCN): 288 nm.

Crystal data: (CCDC-2051221):  $\text{C}_{10}\text{H}_{11}\text{N}_3\text{O}_3$ ; monoclinic;  $a = 5.3717(4)$ ,  $b = 15.2445(12)$ ,  $c = 12.5898(8)$  Å,  $\beta = 91.091(3)^\circ$ ;  $V = 1030.8(2)$  Å $^3$ ;  $Z = 4$ ; space group  $\text{P}2_1/\text{n}$ ;  $T = 120$  K;  $R_1 = 0.052$ .

### Synthesis of 6a–b; General Procedure

(*E*)-2-(3-Acetyl-3-methyltriazol-1-en-1-yl)benzoic acid (0.22 mmol, 0.049 g, 1.0 equiv), and the corresponding azide substrate (0.44 mmol, 2.0 equiv) were dissolved in MeCN (9 mL, 50 mM). The homogeneous stock solution was then passed through the 10 mL coil (3.33 mL/min, residence time 3.0 min) of a Vapourtec E-series photoflow reactor that housed an LED emitting at 365 nm. The temperature was kept constant between 28–30 °C, and pressure was maintained at ca. 2 bar using a backpressure regulator. The emerging product solution was collected in a round-bottom flask prior to being subjected to evaporation of the solvent. All reactions were subsequently purified by flash chromatography (EtOAc/hexanes) to provide the desired product.

#### 1-Benzyl-1-benzo[1,2,3]triazole (6a)

Isolated yield: 66 mg (0.32 mmol, 73%); pale-brown solid; mp 113–115 °C;  $R_f = 0.3$  (25% EtOAc/hexanes).

IR (neat): 3063 (w), 3030 (w), 2990 (w), 2935 (w), 1733 (m), 1712 (m), 1496 (m), 1494 (m)  $\text{cm}^{-1}$ .

$^1\text{H}$  NMR ( $\text{CDCl}_3$ , 400 MHz):  $\delta = 8.06$  (d,  $J = 8.0$  Hz, 1 H), 7.42–7.26 (m, 8 H), 5.84 (s, 2 H).

$^{13}\text{C}$  NMR ( $\text{CDCl}_3$ , 101 MHz):  $\delta = 146.3$  (C), 134.7 (C), 132.8 (C), 128.9 (2x CH), 128.4 (CH), 127.6 (CH), 127.4 (2 x CH), 123.9 (CH), 120.0 (CH), 109.7 (CH), 52.2 ( $\text{CH}_2$ ).

HRMS (TOF-ESI+):  $m/z$  [ $\text{M} + \text{H}$ ] $^+$  calcd for  $\text{C}_{13}\text{H}_{12}\text{N}_3$ : 210.1031; found: 210.1026.

#### 2-(Benzo[1,2,3]triazol-1-yl)-1-phenylethan-1-one (6b)

Isolated yield: 21 mg (0.09 mmol, 56%); dark-yellow oil;  $R_f = 0.4$  (40% EtOAc/hexanes).

IR (neat): 3055 (w), 3029 (w), 2926 (w), 1644 (s), 1466 (m), 1410 (m).

$^1\text{H}$  NMR ( $\text{CDCl}_3$ , 400 MHz):  $\delta = 8.12$ –8.05 (m, 3 H), 7.69–7.65 (m, 1 H), 7.57–7.47 (m, 3 H), 7.42–7.37 (m, 2 H), 6.10 (s, 2 H).

$^{13}\text{C}$  NMR ( $\text{CDCl}_3$ , 101 MHz):  $\delta = 190.3$  (C), 146.1 (C), 134.5 (C), 134.0 (C), 133.8 (CH), 133.5 (CH), 130.1 (CH), 129.2 (CH), 128.3 (CH), 127.8 (CH), 124.1 (CH), 120.2 (CH), 109.5 (CH), 53.9 ( $\text{CH}_2$ ).

HRMS (TOF-ESI+):  $m/z$  [ $\text{M} + \text{H}$ ] $^+$  calcd for  $\text{C}_{14}\text{H}_{11}\text{NaN}_3\text{O}$ : 260.0794; found: 260.0797.

### Synthesis of 6c–f, 10a–f; General Procedure

(*E*)-2-(3-Acetyl-3-methyltriazol-1-en-1-yl)benzoic acid (2.0 equiv) and the corresponding diene/sydnone substrate (1.0 equiv) were dissolved in MeCN (0.1 M, 0.05 M respectively). The homogeneous stock solution was then passed through the 10 mL coil (3.33 mL/min, residence time: 3 min) of a Vapourtec E-series photoflow reactor that housed an LED emitting at 365 nm. The temperature was kept constant between 28–30 °C, and pressure was maintained using a back-

pressure regulator. The resulting product solution was collected in a round-bottom flask prior to evaporation of the solvent. All reactions were subsequently purified by silica gel chromatography to provide the desired product.

#### 1,4-Dihydro-1,4-methanonaphthalene (6c)

Isolated yield: 90 mg (0.63 mmol, 42%); colorless oil.

$^1\text{H}$  NMR ( $\text{CDCl}_3$ , 400 MHz):  $\delta = 7.29$ –7.24 (m, 2 H), 7.07–6.96 (m, 4 H), 5.80 (s, 1 H), 2.40 (s, 3 H).

$^{13}\text{C}$  NMR ( $\text{CDCl}_3$ , 101 MHz):  $\delta = 151.8$  (2C), 142.9 (2CH), 124.2 (2CH), 121.5 (2CH), 70.1 ( $\text{CH}_2$ ), 50.3 (2CH).

#### 1-Methyl-1,4-dihydro-1,4-epoxynaphthalene (6d)

Isolated yield: 31 mg (0.19 mmol, 84%); yellow oil;  $R_f = 0.4$  (15% EtOAc/hexanes).

IR (neat): 3100 (w), 3058 (w), 3032 (w), 2934 (w), 1705 (s), 1744 (s), 1498 (m)  $\text{cm}^{-1}$ .

$^1\text{H}$  NMR ( $\text{CDCl}_3$ , 400 MHz):  $\delta = 7.21$ –7.14 (m, 2 H), 7.03–6.92 (m, 3 H), 6.76 (d,  $J = 8.0$  Hz, 1 H), 5.62 (d,  $J = 4.0$  Hz, 1 H), 1.92 (s, 3 H).

$^{13}\text{C}$  NMR ( $\text{CDCl}_3$ , 101 MHz):  $\delta = 151.3$  (CH), 150.5 (CH), 145.54 (CH), 144.3 (CH), 124.9 (C), 124.7 (C), 119.9 (C), 118.7 (CH), 89.3 (CH), 81.8 (CH), 15.2 ( $\text{CH}_3$ ).

HRMS (TOF-ESI+):  $m/z$  [ $\text{M} + \text{H}$ ] $^+$  calcd for  $\text{C}_{11}\text{H}_{11}\text{O}$ : 159.0804; found: 159.0805.

#### 1-(1,4-Epoxy-naphthalen-1-yl)ethan-1-one (6e)

Isolated yield: 24 mg (0.13 mmol, 57%); pale-yellow oil;  $R_f = 0.3$  (15% EtOAc/hexanes).

IR (neat): 3083 (w), 3061 (w), 3025 (w), 2977 (w), 1743 (s), 1710 (s)  $\text{cm}^{-1}$ .

$^1\text{H}$  NMR ( $\text{CDCl}_3$ , 400 MHz):  $\delta = 7.29$ –7.24 (m, 2 H), 7.07–6.96 (m, 4 H), 5.80 (s, 1 H), 2.40 (s, 3 H).

$^{13}\text{C}$  NMR ( $\text{CDCl}_3$ , 101 MHz):  $\delta = 205.2$  (C), 148.0 (CH), 147.5 (CH), 143.4 (CH), 142.3 (CH), 125.6 (C), 125.2 (C), 120.6 (C), 119.6 (CH), 95.7 (CH), 82.3 (CH), 26.8 ( $\text{CH}_3$ ).

HRMS (TOF-ESI+):  $m/z$  [ $\text{M} + \text{H}$ ] $^+$  calcd for  $\text{C}_{12}\text{H}_{11}\text{O}_2$ : 187.0754; found: 187.0753.

#### 1-(4-Methyl-1,4-epoxynaphthalen-1-yl)ethan-1-one (6f)

Isolated yield: 32 mg (0.16 mmol, 72%); yellow oil;  $R_f = 0.4$  (15% EtOAc/hexanes).

IR (neat): 3085 (w), 3068 (w), 3028 (w), 2981 (w), 1748 (s), 1705 (s)  $\text{cm}^{-1}$ .

$^1\text{H}$  NMR ( $\text{CDCl}_3$ , 400 MHz):  $\delta = 7.19$  (t,  $J = 8.0$  Hz, 2 H), 7.06–6.95 (m, 3 H), 6.77 (d,  $J = 8.0$  Hz, 2 H), 2.39 (s, 3 H), 1.97 (s, 3 H).

$^{13}\text{C}$  NMR ( $\text{CDCl}_3$ , 101 MHz):  $\delta = 205.5$  (C), 150.5 (CH), 149.0 (CH), 145.9 (CH), 143.5 (CH), 125.5 (C), 124.9 (C), 119.1 (C), 119.0 (C), 95.1 (CH), 89.7 (CH), 26.8 ( $\text{CH}_3$ ), 15.1 ( $\text{CH}_3$ ).

HRMS (TOF-ESI+):  $m/z$  [ $\text{M} + \text{H}$ ] $^+$  calcd for  $\text{C}_{13}\text{H}_{13}\text{O}_2$ : 201.0910; found: 201.0911.

#### 2,3-Dihydro-1-pyrrolo[1,2]indazole (10a)<sup>18d</sup>

Isolated yield: 648 mg (4.1 mmol, 68%); off-white solid; mp 98–100 °C;  $R_f = 0.3$  (50%  $\text{CH}_2\text{Cl}_2/\text{EtOAc}$ ).

IR (neat): 3023 (w), 2983 (w), 2890 (w), 1746 (s), 1713 (s)  $\text{cm}^{-1}$ .

<sup>1</sup>H NMR (CDCl<sub>3</sub>, 400 MHz): δ = 7.64 (d, *J* = 8.0 Hz, 1 H), 7.54 (d, *J* = 8.0 Hz, 1 H), 7.23 (t, *J* = 8.0 Hz, 1 H), 7.01 (t, *J* = 8.0 Hz, 1 H), 4.39 (t, *J* = 8.0 Hz, 2 H), 3.15 (t, *J* = 8.0 Hz, 2 H), 2.70 (app p, *J* = 8.0 Hz, 2 H).

<sup>13</sup>C NMR (CDCl<sub>3</sub>, 101 MHz): δ = 153.7 (C), 138.8 (C), 125.6 (CH), 120.4 (CH), 119.8 (CH), 117.7 (CH), 116.2 (C), 48.9 (CH<sub>2</sub>), 25.8 (CH<sub>2</sub>), 23.0 (CH<sub>2</sub>).

HRMS (TOF-ESI+): *m/z* [M + H]<sup>+</sup> calcd for C<sub>10</sub>H<sub>11</sub>N<sub>2</sub>: 159.0917; found: 159.0916.

Crystal data: (CCDC-2051222): C<sub>10</sub>H<sub>10</sub>N<sub>2</sub>; monoclinic; *a* = 6.6759(3), *b* = 17.5344(8), *c* = 7.3037(3) Å, β = 108.476(2)°; *V* = 810.89(6) Å<sup>3</sup>; *Z* = 4; space group P2<sub>1</sub>/n; *T* = 120 K; *R*<sub>1</sub> = 0.054.

### 2-Phenyl-2H-indazole (10b)<sup>18d</sup>

Isolated yield: 32 mg (0.17 mmol, 77%); yellow solid; 82–84 °C; *R*<sub>f</sub> = 0.4 (10% EtOAc/hexanes).

IR (neat): 3130 (w), 3054 (w), 1628 (w), 1592 (m), 1518 (s), 1494 (s) cm<sup>-1</sup>.

<sup>1</sup>H NMR (CDCl<sub>3</sub>, 400 MHz): δ = 8.40 (d, *J* = 1.2 Hz, 1 H), 7.89 (dd, *J* = 8.6, 1.2 Hz, 2 H), 7.80–7.76 (m, 1 H), 7.70 (d, *J* = 8.6 Hz, 1 H), 7.51 (dd, *J* = 8.7, 7.2 Hz, 2 H), 7.41–7.36 (m, 1 H), 7.31 (ddd, *J* = 8.9, 6.6, 1.1 Hz, 1 H), 7.14–7.07 (m, 1 H).

<sup>13</sup>C NMR (CDCl<sub>3</sub>, 101 MHz): δ = 149.8 (C), 140.5 (C), 129.6 (2CH), 127.9 (CH), 126.8 (CH), 122.8 (C), 122.5 (CH), 121.0 (2CH), 120.4 (CH), 120.4 (CH), 117.9 (CH).

HRMS (TOF-ESI+): *m/z* [M + H]<sup>+</sup> calcd for C<sub>13</sub>H<sub>11</sub>N<sub>2</sub>: 195.0917; found: 195.0928.

### 2-(*p*-Tolyl)-2H-indazole (10c)<sup>18d</sup>

Isolated yield: 38 mg (0.18 mmol, 82%); yellow solid; 99–101 °C; *R*<sub>f</sub> = 0.4 (10% EtOAc/hexanes).

IR (neat): 3133 (w), 3054 (w), 2915 (w), 2859 (w), 1627 (w), 1523 (s) cm<sup>-1</sup>.

<sup>1</sup>H NMR (CDCl<sub>3</sub>, 400 MHz): δ = 8.37 (s, 1 H), 7.81–7.77 (m, 3 H), 7.71 (dt, *J* = 8.0, 4.0 Hz, 1 H), 7.34–7.30 (m, 3 H), 7.12 (ddd, *J* = 8.4, 6.8, 0.8 Hz, 1 H), 2.43 (s, 3 H).

<sup>13</sup>C NMR (CDCl<sub>3</sub>, 100 MHz): δ = 149.6 (C), 138.3 (C), 137.9 (C), 130.1 (2CH), 126.6 (CH), 122.7 (C), 122.3 (CH), 120.9 (2CH), 120.3 (CH), 120.3 (CH), 117.8 (CH), 21.0 (CH<sub>3</sub>).

HRMS (TOF-ESI+): *m/z* [M + H]<sup>+</sup> calcd for C<sub>14</sub>H<sub>13</sub>N<sub>2</sub>: 209.1073; found: 209.1069.

### 2-(4-Methoxyphenyl)-2H-indazole (10d)<sup>18d</sup>

Isolated yield: 48 mg (0.23 mmol, 79%); yellow solid; mp 130–132 °C; *R*<sub>f</sub> = 0.4 (15% EtOAc/hexanes).

IR (neat): 3137 (w), 3053 (w), 3012 (m), 2837 (m), 1519 (s), 1244 (s) cm<sup>-1</sup>.

<sup>1</sup>H NMR (CDCl<sub>3</sub>, 400 MHz): δ = 8.31 (s, 1 H), 7.82–7.78 (m, 3 H), 7.70 (dt, *J* = 8.8, 1.2 Hz, 1 H), 7.32 (ddd, *J* = 8.4, 6.4, 0.8 Hz, 1 H), 7.11 (ddd, *J* = 8.4, 6.4, 0.8 Hz, 1 H), 7.02 (d, *J* = 8.0 Hz, 2 H), 3.87 (s, 3 H).

<sup>13</sup>C NMR (CDCl<sub>3</sub>, 101 MHz): δ = 159.3 (C), 149.6 (C), 134.1 (C), 126.5 (CH), 122.7 (C), 122.4 (2CH), 122.2 (CH), 120.3 (CH), 120.2 (CH), 117.8 (CH), 114.6 (2CH), 55.6 (CH<sub>3</sub>).

HRMS (TOF-ESI+): *m/z* [M + H]<sup>+</sup> calcd for C<sub>14</sub>H<sub>13</sub>N<sub>2</sub>O: 225.1022; found: 225.1024.

### 2-(4-Isopropylphenyl)-2H-indazole (10e)

Isolated yield: 40 mg (0.17 mmol, 70%); yellow solid; mp 90–92 °C; *R*<sub>f</sub> = 0.5 (15% EtOAc/hexanes).

IR (neat): 3054 (w), 2958 (m), 2867 (w), 1628 (w), 1522 (s) cm<sup>-1</sup>.

<sup>1</sup>H NMR (CDCl<sub>3</sub>, 400 MHz): δ = 8.38 (s, 1 H), 7.83–7.79 (m, 3 H), 7.71 (dt, *J* = 8.8, 1.2 Hz, 1 H), 7.40–7.36 (m, 2 H), 7.32 (ddd, *J* = 8.8, 6.8, 0.8 Hz, 1 H), 7.11 (ddd, *J* = 8.8, 6.8, 0.8 Hz, 1 H), 2.99 (m, 1 H), 1.31 (d, *J* = 8.0 Hz, 6 H).

<sup>13</sup>C NMR (CDCl<sub>3</sub>, 101 MHz): δ = 149.7 (C), 148.9 (C), 138.5 (C), 127.5 (2 × CH), 126.6 (CH), 122.7 (C), 122.3 (CH), 121.0 (2 × CH), 120.3 (CH), 120.3 (CH), 117.9 (CH), 33.8 (CH), 23.9 (2CH<sub>3</sub>).

HRMS (TOF-ESI+): *m/z* [M + H]<sup>+</sup> calcd for C<sub>16</sub>H<sub>17</sub>N<sub>2</sub>: 237.1386; found: 237.1383.

### 2-(3,4-Dichlorophenyl)-2H-indazole (10f)

Isolated yield: 8 mg (0.03 mmol, 18%); white solid; mp 127–129 °C; *R*<sub>f</sub> = 0.3 (10% EtOAc/hexanes).

IR (neat): 3131 (w), 3100 (w), 3059 (w), 1629 (w), 1519 (s), 1485 (s) cm<sup>-1</sup>.

<sup>1</sup>H NMR (CDCl<sub>3</sub>, 600 MHz): δ = 8.38 (s, 1 H), 8.10 (d, *J* = 4.0 Hz, 1 H), 7.78–7.75 (m, 2 H), 7.70 (d, *J* = 4.0 Hz, 1 H), 7.60 (d, *J* = 4.0 Hz, 1 H), 7.34 (ddd, *J* = 9.6, 7.2, 1.2 Hz, 1 H), 7.13 (ddd, *J* = 9.6, 7.2, 1.2 Hz, 1 H).

<sup>13</sup>C NMR (CDCl<sub>3</sub>, 151 MHz): δ = 150.1 (C), 139.6 (C), 133.8 (C), 131.8 (C), 131.2 (CH), 127.5 (CH), 123.1 (CH), 123.0 (C), 122.6 (CH), 120.4 (CH), 120.3 (CH), 119.6 (CH), 118.0 (CH).

HRMS (TOF-ESI+): *m/z* [M + H]<sup>+</sup> calcd for C<sub>13</sub>H<sub>9</sub>Cl<sub>2</sub>N<sub>2</sub>: 263.0137; found: 263.0139.

## Funding Information

This research has been enabled through funding by SSPC (European Regional Development Fund; 12/RC2275\_P2) and instrumentation acquired through a recent Science Foundation Ireland Infrastructure Call 2018 (18/RI/5702). We gratefully acknowledge support from the School of Chemistry at UCD for a PhD scholarship (to CB). Support of our research through a RSC Research Enablement Grant (E20-2998 to MB) is acknowledged.

## Supporting Information

Supporting information for this article is available online at <https://doi.org/10.1055/s-0040-1706016>.

## References

- (1) (a) Gutmann, B.; Cantillo, D.; Kappe, C. O. *Angew. Chem. Int. Ed.* **2015**, *54*, 6688. (b) Movsisyan, M.; Delbeke, E. I. P.; Berton, J. K. E. T.; Battilocchio, C.; Ley, S. V.; Stevens, C. V. *Chem. Soc. Rev.* **2016**, *45*, 4892. (c) Baumann, M.; Moody, T. S.; Smyth, M.; Wharry, S. *Org. Process Res. Dev.* **2020**, *23*, 1802. (d) Dallinger, D.; Gutmann, B.; Kappe, C. O. *Acc. Chem. Res.* **2020**, *53*, 1330.
- (2) (a) Colella, M.; Nagaki, A.; Luisi, R. *Chem. Eur. J.* **2020**, *26*, 19. (b) Baumann, M.; Moody, T. S.; Smyth, M.; Wharry, S. *Eur. J. Org. Chem.* **2020**, 7398.
- (3) (a) Sambiagio, C.; Noël, T. *Trends Chem.* **2020**, *2*, 92. (b) Di Filippo, M.; Bracken, C.; Baumann, M. *Molecules* **2020**, *25*, 356. (c) Elliott, L. D.; Knowles, J. P.; Koovits, P. J.; Maskil, K. G.; Ralph,

- M. J.; Lejeune, G.; Edwards, L. J.; Robinson, R. I.; Clemens, I. R.; Cox, B.; Pascoe, D. D.; Koch, G.; Eberle, M.; Berry, M. B.; Booker-Milburn, K. I. *Chem. Eur. J.* **2014**, *20*, 15226.
- (4) Rehm, T. H. *ChemPhotoChem* **2020**, *4*, 235.
- (5) For selected recent examples, see: (a) Steiner, A.; Roth, P. M. C.; Strauss, F. J.; Gauron, G.; Tekautz, G.; Winter, M.; Williams, J. D.; Kappe, C. O. *Org. Process Res. Dev.* **2020**, *24*, 2208. (b) Levesque, F.; Di Maso, M. J.; Narsimhan, K.; Wismer, M. K.; Naber, J. R. *Org. Process Res. Dev.* **2020**, *24*, 2935. (c) Williams, J. D.; Nakano, M.; Gerardy, R.; Rincon, J. A.; de Frutos, O.; Mateos, C.; Monbaliu, J.-C. M.; Kappe, C. O. *Org. Process Res. Dev.* **2019**, *23*, 78. (d) Alcazar, J.; Abdiaj, I. *Bioorg. Med. Chem.* **2017**, *25*, 6190. (e) Cochran, J. E.; Waal, N. *Org. Process Res. Dev.* **2016**, *20*, 1533.
- (6) (a) Levesque, F.; Seeberger, P. H. *Angew. Chem. Int. Ed.* **2012**, *51*, 1706. (b) Kopetzki, D.; Levesque, F.; Seeberger, P. H. *Chem. Eur. J.* **2013**, *19*, 5450. (c) Turconi, J.; Griollet, F.; Guevel, R.; Oddon, G.; Villa, R.; Geatti, A.; Hvala, M.; Rossen, K.; Göller, R.; Burgard, A. *Org. Process Res. Dev.* **2014**, *18*, 417. (d) Triemer, S.; Gilmore, K.; Vu, G. T.; Seeberger, P. H.; Seidel-Morgenstern, A. *Angew. Chem. Int. Ed.* **2018**, *57*, 5525.
- (7) For previous reports on generating benzynes in flow, see: (a) Browne, D. L.; Wright, S.; Deadman, B. J.; Dunnage, S.; Baxendale, I. R.; Turner, R. M.; Ley, S. V. *Rapid Commun. Mass Spectrom.* **2012**, *26*, 1999. (b) Nagaki, A.; Ichinari, D.; Yoshida, J. *J. Am. Chem. Soc.* **2014**, *136*, 12245. (c) Susanne, F.; Martin, B.; Aubry, M.; Sedelmeier, J.; Lima, F.; Sevinc, S.; Piccioni, L.; Haber, J.; Schenkel, B.; Venturoni, F. *Org. Process Res. Dev.* **2017**, *21*, 1779. (d) Tan, Z.; Li, Z.; Jin, G.; Yu, C. *Org. Process Res. Dev.* **2019**, *23*, 31.
- (8) Himenshima, Y.; Sonoda, T.; Kobayashi, H. *Chem. Lett.* **1983**, *12*, 1211.
- (9) (a) Wenk, H. H.; Winkler, M.; Sander, W. *Angew. Chem. Int. Ed.* **2003**, *42*, 502. (b) Takikawa, H.; Nishii, A.; Sakaib, T.; Suzuki, K. *Chem. Soc. Rev.* **2018**, *47*, 8030. (c) Pellissier, H.; Santelli, M. *Tetrahedron* **2003**, *59*, 701.
- (10) Goetz, A. E.; Garg, N. K. *J. Org. Chem.* **2014**, *79*, 846; and references therein.
- (11) Chang, D.; Zhu, D.; Shi, L. *J. Org. Chem.* **2015**, *80*, 5928.
- (12) (a) Maki, Y.; Furuta, T.; Suzuki, M. *J. Chem. Soc., Perkin Trans. 1979*, *1*, 553. (b) Maki, Y.; Furuta, T.; Kuzuya, M.; Suzuki, M. *J. Chem. Soc., Chem. Commun.* **1975**, 616.
- (13) Gann, A. W.; Amoroso, J. W.; Einck, V. J.; Rice, P. W.; Chambers, J. J.; Schnarr, N. A. *Org. Lett.* **2014**, *16*, 2003.
- (14) CCDC 2051221 contains the supplementary crystallographic data for this paper. The data can be obtained free of charge from The Cambridge Crystallographic Data Centre via [www.ccdc.cam.ac.uk/structures](http://www.ccdc.cam.ac.uk/structures).
- (15) For recent examples, see: (a) Bonciolini, S.; Di Filippo, M.; Baumann, M. *Org. Biomol. Chem.* **2020**, *18*, 9428. (b) Di Filippo, M.; Baumann, M. *Eur. J. Org. Chem.* **2020**, 6199. (c) Laudadio, G.; Deng, Y.; van der Wal, K.; Ravelli, D.; Nuno, M.; Fagnoni, M.; Guthrie, D.; Sun, Y.; Noël, T. *Science* **2020**, *369*, 92.
- (16) Briguglio, I.; Piras, S.; Corona, P.; Gavini, E.; Nieddu, M.; Boatto, G.; Carta, A. *Eur. J. Org. Chem.* **2015**, 612.
- (17) (a) Zhang, S.-G.; Liang, C.-G.; Zhang, W.-H. *Molecules* **2018**, *23*, 2738. (b) Cerecetto, H.; Gerpe, A.; Gonzalez, M.; Aran, V.; de Ocariz, C. *Mini-Rev. Med. Chem.* **2005**, *5*, 869. (c) Gaikwad, D. D.; Chapolikar, A. D.; Devkate, C. G.; Warad, K. D.; Tayade, A. P.; Pawar, R. P.; Domb, A. J. *Eur. J. Med. Chem.* **2015**, *90*, 707.
- (18) (a) Applegate, J.; Turnbull, K. *Synthesis* **1988**, 1011. (b) Azarifar, D.; Ghasemnejad-Borsa, H. *Synthesis* **2006**, 1123. (c) Browne, D. L.; Vivat, J. F.; Plant, A.; Gomez-Bengoa, E.; Harrity, J. P. A. *J. Am. Chem. Soc.* **2009**, *131*, 7762. (d) Fang, Y.; Wu, C.; Larock, R. C.; Shi, F. *J. Org. Chem.* **2011**, *76*, 8840.
- (19) Larock and co-workers observed a similar outcome using 4-nitrophenyl sydnone when no 2H-indazole product was isolated, whereas monochlorinated benzene appendages were tolerated, see reference 18d.
- (20) CCDC 2051222 contains the supplementary crystallographic data for this paper. The data can be obtained free of charge from The Cambridge Crystallographic Data Centre via [www.ccdc.cam.ac.uk/structures](http://www.ccdc.cam.ac.uk/structures).
- (21) The high-power LED system used in this study is available from Vapourtec (<https://www.vapourtec.com/>).